Analysis of Ambient Noise Spectrum Level Correlation Characteristics in the China Sea

JIANBO ZHOU [iD]

School of Marine Science and Technology, Northwestern Polytechnical University, Xi'an 710072, China
Key Laboratory of Ocean Acoustics and Sensing, Ministry of Industry and Information Technology, Northwestern Polytechnical University, Xi'an 710072, China
State Key Laboratory of Acoustic, Institute of Acoustic, Chinese Academy of Sciences, Beijing 100190, China

e-mail: jbzhou@nwpu.edu.cn

ABSTRACT The ambient noise field in the ocean is formed by a mixture of many source types, such as seismic noise, marine noise, shipping noise, and wind-generated noise. The correlation matrices of the ambient noise spectrum levels offer a promising approach for identifying and isolating the active source mechanisms in ambient noise datasets. This study attempts to use frequency correlation matrices to examine inter-frequency relationships and identify frequency bands that are dominated by specific sources present in samples of ambient noise. Deep-ocean ambient noise recorded by hydroacoustic monitoring systems in the East China Sea and South China Sea was used to analyze the frequency correlation characteristics over a broadband frequency range, with a focus on the contribution of wind-related and shipping-related source mechanisms to the overall ambient noise field at various frequencies. The primary sources observed in both the South China Sea and East China Sea were shipping sources and wind sources. During the observation window, wind was responsible for a significant amount of the ambient noise energy above 477 Hz in the East China Sea, while the corresponding frequency threshold was shifted up to 575 Hz in the South China Sea. Another interesting feature was also observed in the East China Sea: a higher degree of correlation was found between the levels at the wind noise dominated frequencies and mixture noise (mainly consisting of wind noise and shipping noise) dominated frequencies at the upper receiver than at the lower receiver. Data analysis results show that the cause of this effect is that shipping activity contributes more to the soundscape at the lower receiver than at the upper receiver.

INDEX TERMS Ambient noise, correlation matrices, wind-related noise, shipping-related noise.

I. INTRODUCTION

The spectral characteristics of ambient noise in the deep ocean are continually changing due to changes in the nature and positions of the many sources that contribute to it [1] as well as the fluctuations in transmission associated with varying oceanographic conditions [2]–[5]. Understanding the variability of ambient noise in the ocean is essential for investigating natural ocean processes such as wind [6]–[12], submarine seismic activity [13]–[16], and breaking waves [17]–[20] as well as for monitoring anthropogenic activities such as oil exploration [21] and marine transport [22]–[26].

The associate editor coordinating the review of this manuscript and approving it for publication was Emrecan Demirors [iD].

Correlation matrices are a useful tool for visually identifying different variables that tend to change together. And the correlation matrices have been effectively researched in many fields [27]–[29], a number of studies have attempted to adapt it for use in underwater ambient noise analysis in recently years. The earliest known analysis of underwater ambient noise by means of correlating the sound levels in different frequency bands was performed by Nichols and Sayer [30]. In their work, they used a 4.5-day recording of ambient noise from a bottom-mounted receiver in the Atlantic Ocean and correlated the sound levels of seven different frequency band pairs, with band center frequencies ranging from 5 to 150 Hz. A high degree of correlation was found between the levels at low frequencies (5-25 Hz) and those at high frequencies (70-150 Hz), while

the primary midrange frequencies (25-70) were poorly correlated with both the lower and higher frequencies. The data analysis results showed that the causes of these effects were the dominance of wind noise at high and low frequencies and the dominance of shipping noise in the middle range.

Curtis *et al.* [31] found similar results by computing the covariance of the spectral levels at pairs of frequencies based on long-term ambient noise statistics collected by 13 widely distributed receivers in the North Pacific. For some receivers, the sound level in the 12-15 Hz band was moderately correlated with the sound level in the 200-400 Hz band, indicating that both of these frequency bands are associated with wind events. In addition, an interesting acoustical phenomenon was observed in which the correlation between the sound level in the 200-400 Hz band and the wind speed was weaker for the coastal ocean than for the open ocean.

Using low-frequency deep ocean ambient noise data recorded by the Comprehensive Nuclear-Test-Ban Treaty Organization (CTBTO) hydroacoustic monitoring system, Nichols and Bradley et al. performed a series of studies using the correlation matrix technique. In 2013, they [32] applied this technique to identify and isolate sources present in large low-frequency ambient noise datasets and successfully identified microseism, earthquake, airgun and whale noise from deep ocean data. In addition, they [33] investigated the relationship between the wind speed and the sound levels in different frequency bands to determine the prominence of wind-related noise in the combined ambient noise spectrum. In 2014, they [34] extended the use of correlation matrices to the identification of the temporal characteristics of underwater ambient noise sources. The correlation matrices were computed for two groups of noise spectra, grouped by two different surface wind speed categories. After an exhaustive analysis of the measured ambient noise data, they drew the following conclusions: the noise spectrum under low wind conditions (≤2 knots) did not reach saturation until approximately 4 Hz, while the noise levels were unsaturated up to 2 Hz for high wind speeds (5-25 knots). In 2015, they [35] briefly discussed the possible applications of the correlation matrix technique for three purposes: to analyze the change of ambient noise with time, to monitor meteorological conditions in remote locations, and to better define the source properties of ambient noise. The ability to use correlation matrices to identify active sound sources was also further exploited by Miksis-Olds and Nichols in 2016 [36], by analyzing the primary drivers behind multiyear changes in ambient noise levels, these authors provided a reasonable explanation for the decreasing trend in low-frequency noise (5-115 Hz) in the Equatorial Pacific and South Atlantic Oceans observed in recent years. An exhaustive discussion of correlation matrices for ambient noise is presented in [37], in which the use of correlation matrices is extended to the identification of characteristic spectra of specific sources to enable the use of a limited number of those spectra to reconstruct measured ambient noise fields.

As discussed above, frequency correlation matrices have proven useful in identifying the underlying frequency structures and constituent sound spectra of measured noise. This study attempts to identify frequency bands which are dominated by specific sources present in samples of ambient noise recorded in the South China Sea and East China Sea using frequency correlation matrices. The dominant frequencies of wind noise and shipping noise at two experimental sites are analyzed and compared, and the influence of wind speed conditions and the receiving depth on the frequency correlation characteristics at various frequencies is investigated.

This paper is organized as follows. A brief description of the theory of frequency noise correlation is given in Sec. II, followed in Sec. III by a detailed introduction to the relevant data acquisition and processing procedures. Spectrograms from various receivers and the associated frequency correlation matrices are presented, and the dominant sources at various frequencies are identified using the noise correlation technique. The proportion of wind activity contributing to the soundscape at different receiving depths is investigated by comparing the spectral correlations at different receiving depths. The final section summarizes the key results.

II. THEORY OF NOISE FREQUENCY CORRELATION

Correlation matrices reveal critical information about the relationships between groups of measured variables. For the present analysis, the variables are the characteristics of the frequency spectrum. Frequency correlation matrices are useful for better identifying and understanding changes in the contributions of different sources to regional soundscapes. The normalized correlation coefficient between the demeaned spectral densities (in dB) at frequencies f_c and f_d is defined as follows:

$$r\left(f_c, f_d\right)$$
$$= \frac{\sum_{a=1}^{N}\left(X\left(f_c, t_a\right) - \overline{X\left(f_c\right)}\right)\left(X\left(f_d, t_a\right) - \overline{X\left(f_d\right)}\right)}{\sqrt{\sum_{a=1}^{N}\left(X\left(f_c, t_a\right) - \overline{X\left(f_c\right)}\right)^2 \sum_{a=1}^{N}\left(X\left(f_d, t_a\right) - \overline{X\left(f_d\right)}\right)^2}}$$

(1)

Here, $X\left(f_c, t_a\right)$ represents the spectral density at frequency band f_c using the ath time segment, whereas the overbar represents the mean over all times, and N is the number of time segments. High correlation between the sound levels at a given pair of frequencies indicates that the corresponding sound levels tend to increase and decrease at the same time, implying that the noise at this pair of frequencies is likely due to the same source mechanism. Similarly, a large frequency region in which the sound levels are strongly correlated indicates a frequency range in which the noise is due to a particular source. The strength of the correlation coefficients in the matrix is predominantly driven by the amplitudes of the source signals relative to the background noise and the durations of the signals relative to the total length of the analysis window [34].

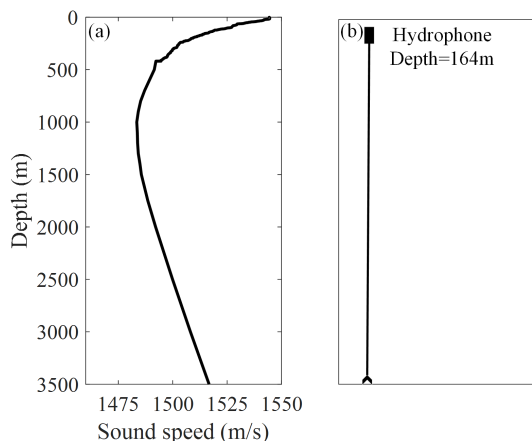The frequency correlation matrix of a measured noise recording is constructed via the following steps: First,

FIGURE 1. (a) Measured sound speed profile and (b) illustration of the receiving system for the experiment in the South China Sea.

the total recording is discretized into N time segments $x(t_a)$, $t_a \in t_1, t_2 \ldots t_N$, and those segments are converted into a series of sound pressure spectra $X(f_c, t_a)$, $f_c \in f_1, f_2 \ldots, f_M$ using the Fast Fourier transform (FFT). Second, the spectral densities for all windows are averaged to obtain the mean spectral density at each frequency. In the third step, the correlation coefficients for arbitrary pairs of frequencies are obtained using the above equation. The chosen lengths of the FFT windows and averaging segments will be specified in detail in the data processing descriptions given in the latter section.

III. DATA AND ANALYSIS

A. THE SOUTH CHINA SEA EXPERIMENT

1) DESCRIPTION OF THE EXPERIMENT AND DATA PROCESSING

The analysis data used here were obtained from measurements in the South China Sea. Fig. 1 shows the measured sound speed profile and a schematic diagram of the subsurface mooring used in the experiment. The sound channel axis was at a depth of approximately 1000 m, and a sound pressure receiver was deployed at a depth of 164 m. The sampling frequency for the sound pressure recordings was 12000 Hz to provide information at acoustic frequencies up to 6000 Hz. Information from the receiver response curves was applied to the data to obtain absolute values over the full frequency spectrum. The dataset selected for this study has a duration of approximately 10 hours. Fig. 6 (b) shows the spectrogram for that time period, consisting of 1200 time segments, each of 30 seconds in length. For Fig. 2, Fig. 3 and Fig. 5, to achieve a high frequency resolution at a relatively low computational cost, the recorded data were first downsampled to 1600 Hz before data analysis, and the spectral levels were then calculated using a Hann-windowed 6400-point discrete Fourier transform with no overlap to produce sequential 30-second mean power spectrum estimates over the duration of the dataset. With this design, the frequency resolution is 0.25 Hz, and the time resolution
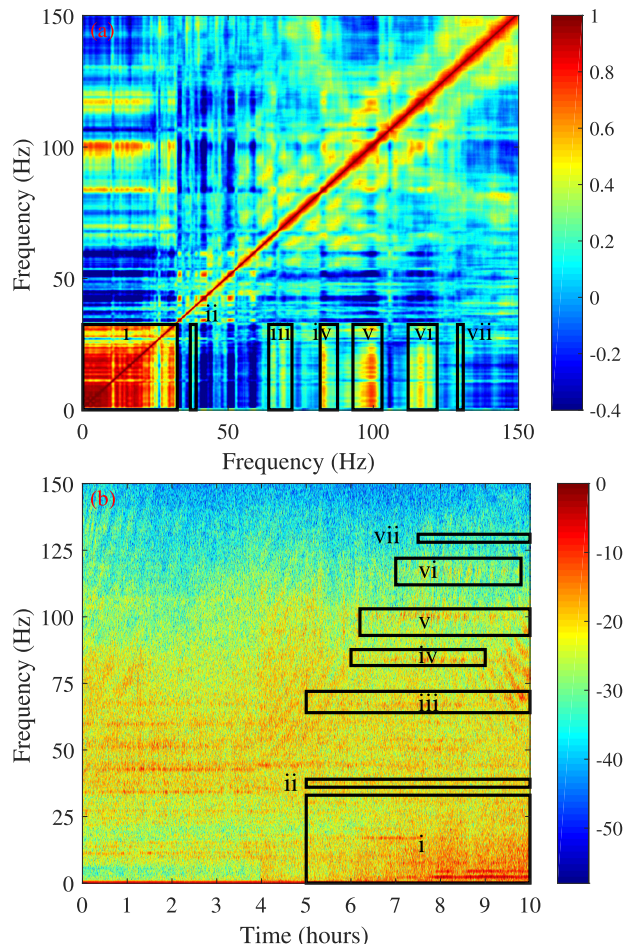

FIGURE 2. (a) Frequency correlation matrix and (b) corresponding spectrogram of the ambient noise in the 0-150 Hz band recorded in the South China Sea. The spectrogram has been normalized by subtracting the maximum spectral densities.

is 30 seconds. For Fig. 6, the spectral levels were calculated using a Hann-windowed 12000-point discrete Fourier transform without downsampling preprocessing, this discretization results in a frequency resolution of 1 Hz and a time resolution of 30 seconds.

2) CORRELATION MATRIX ANALYSIS

Fig. 2 (a) illustrates the frequency correlation matrix of the set of ambient noise data in the 0-150 Hz band, and the corresponding spectrogram is shown in Fig. 2 (b). The spectrogram has been normalized by subtracting the maximum spectral densities. As one might expect, the diagonal elements are always exactly unity, and there is a general tendency for the correlations of the levels at a given frequency f_1 with the levels at various other frequencies f_2 to fall off as the frequency spacing between f_1 and f_2 increases in either direction. Two other features can be observed. First, a broadband feature from 2 to 33 Hz is observed in approximately the last six hours of the dataset [region (i) of Fig. 2 (b)]. The amplitude of this feature is constant across the bandwidth and varies randomly over time. This feature corresponds to an unknown
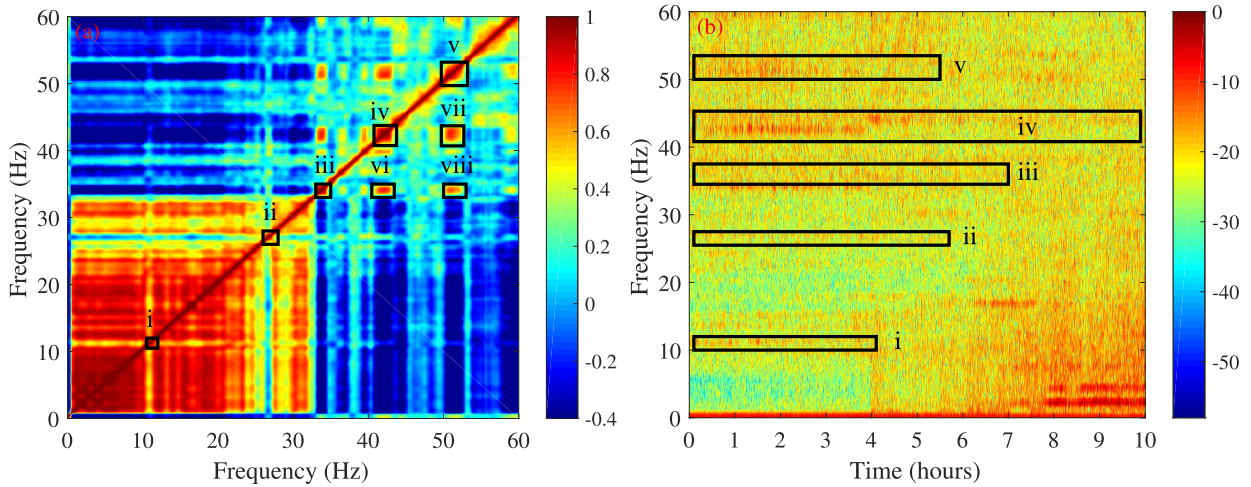
FIGURE 3. (a) Frequency correlation matrix and (b) corresponding spectrogram of the ambient noise in the 0-60 Hz band recorded in the South China Sea. The spectrogram has been normalized by subtracting the maximum spectral densities.
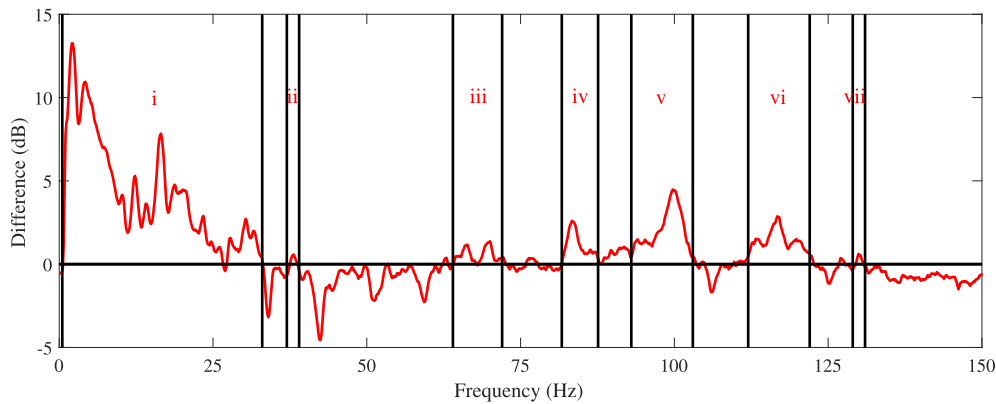

FIGURE 4. The difference in the average sound levels between the last five hours and the first five hours in the 0-10 Hz band. All spectral levels are reported in dB re $1Pa^2/Hz$.

source mechanism and results in a block of strong correlation from 2 to 33 Hz, which ends abruptly at 2 and 33 Hz; the corresponding correlation behavior shows sharp transitions at those two frequencies, implying that the dominant sources change beyond this frequency band. In addition, a set of narrowband tones is also present during the last five hours, with frequency ranges of 37-39 Hz, 64-72 Hz, 81-87 Hz, 93-103 Hz, 112-122 Hz and 129-131 Hz, corresponding to the regions labeled (ii) to (vii) in Fig. 2 (b). The average amplitudes of these narrowband tones range from 0.1 to 4.8 dB above the background. The sound levels in these narrowband tone dominated regions are moderately well correlated ($r = 0.3$-0.75) with the sound levels in the frequency range dominated by the broadband feature, as shown in regions (ii) to (vii) of Fig. 2(a).

The frequency correlation matrix of the ambient noise dataset in the 0-60 Hz band is shown in Fig. 3 (a), and the corresponding spectrogram is presented in Fig. 3 (b). Five narrowband tones are detected, which mainly appear in the first five hours, corresponding to region (i) to (v) in Fig. 3 (b). These features are representative of distant shipping noise. The first two narrowband tones are fully contained within

the frequency limits of the unknown source corresponding to region (i) in Fig. 2 (a) but are independent of that feature, as reflected in the frequency correlation matrix. These two features create a band of strong correlation from 10.5 to 12 Hz and 26 to 27.5 Hz, but uncorrelated from the surrounding region, resulting in two "plus-sign"-shaped correlation feature, labeled as regions (i) and (ii) in Fig. 3 (a). The square regions of high correlation labeled (iii) to (v) in Fig. 3(a) represent the other three narrowband tones, corresponding to regions (iii) to (v) in Fig. 3 (b). Another noticeable feature is that these three narrowband tones translate to an additional series of moderate correlation rectangles in the correlation matrix, representing the correlations between the different narrowband tone pairs. The side lengths of these rectangles, labeled as regions (vi) to (viii) in Fig. 3 (a), are equal to the widths of the frequency bands of each corresponding pair of narrowband tones. Notably, the soundscape was mainly dominated by the features labeled (i) to (v) in Fig. 3 for the first five hours but was mainly dominated by the features labeled (i) to (v) in Fig. 2 for the last five hours, as shown in Fig. 4. Since these two clusters of features generally appeared in different time periods, the correlation between them is weak.
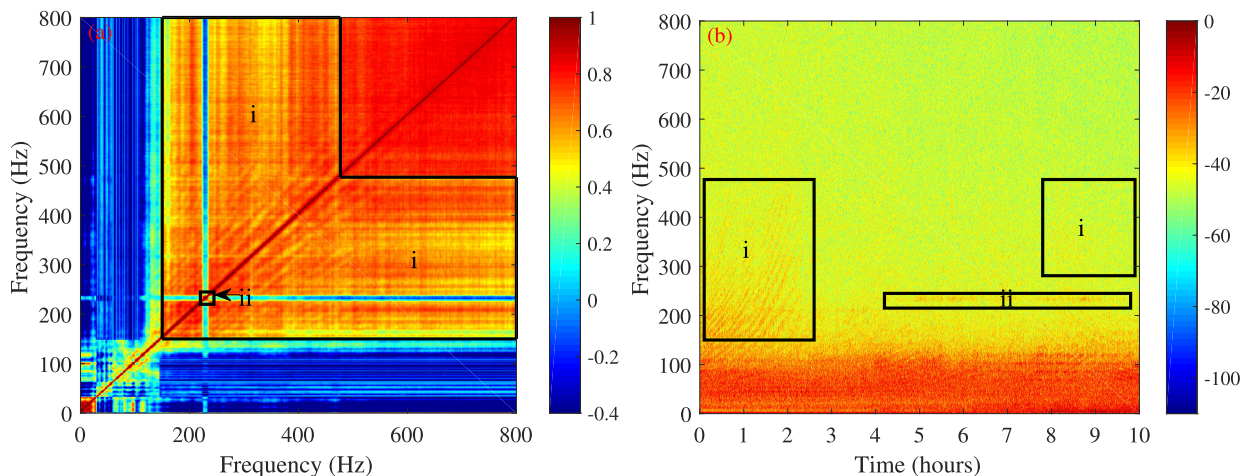
FIGURE 5. (a) Frequency correlation matrix and (b) corresponding spectrogram of the ambient noise in the 1-800 Hz band recorded in the South China Sea. The spectrogram has been normalized by subtracting the maximum spectral densities.
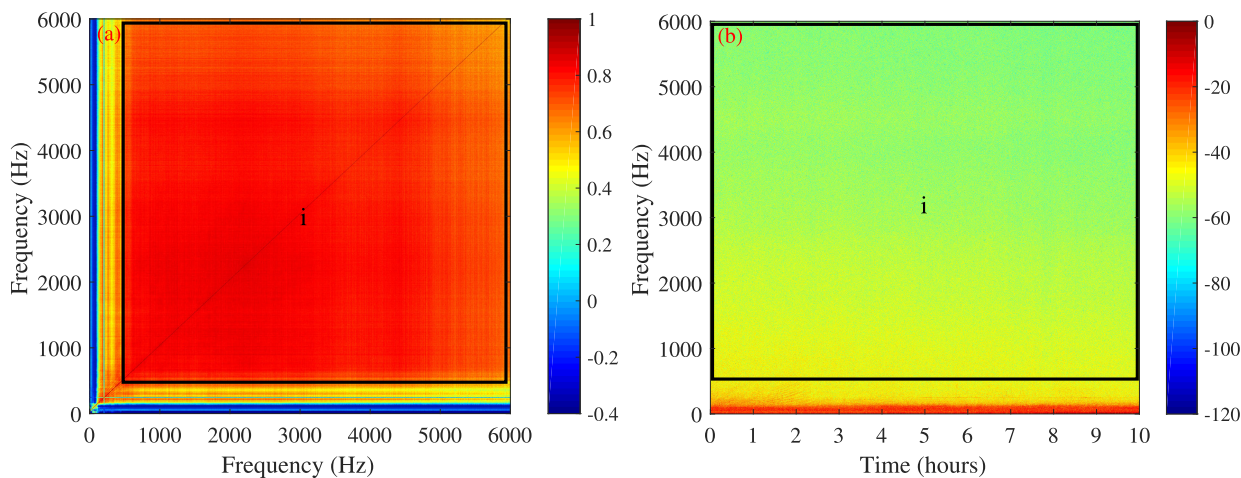

FIGURE 6. (a) Frequency correlation matrix and (b) corresponding spectrogram of the ambient noise in the 1-6000 Hz band recorded in the South China Sea. The spectrogram has been normalized by subtracting the maximum spectral densities.

In Fig.4, the average sound level $\tilde{X}$ at frequency f is defined as:

$$\tilde{X}(f) = \frac{1}{K}\sum_{k=1}^{K}X(f,t_k) \qquad (2)$$

Fig. 5 (a) illustrates the frequency correlation matrix of the ambient noise data in the 0-800 Hz band, and the corresponding spectrogram is shown in Fig. 5 (b). The spectrogram contains two prominent spectral features. First, two strong broadband components are evident, which was present during the first 2.5 hours (with the energy concentrated above 150 Hz) and the last two hours (with the energy concentrated between approximately 290 and 477 Hz), as seen in the two regions labeled (i) in Fig. 5 (b). This feature corresponds to ships passing in the vicinity. The classical work of Wenz [38] indicates that the ambient noise at frequencies from dozens of Hertz to several hundred Hertz in deep water near a sea route is a mixture of wind noise and nearby discrete shipping noise. Thus, it is reasonable to expect that the ambient noise

in the 150 to 477 Hz band is dominated by a mixture of wind noise and nearby discrete shipping noise during the observation period. This translates to a square region of moderate correlation (average correlation coefficient $r = 0.61$) from 150 to 470 Hz in region (i) of Fig. 5 (a). Since wind sources make a nonnegligible contribution to the soundscape in the 150-477 Hz range, the sound levels in that range are moderately well correlated (average correlation coefficient $r = 0.56$) with the sound levels in the frequency range dominated by wind noise (above 477 Hz). Second, a narrowband harmonic tone was persistently present during the last 5.5 hours, with a frequency range of approximately 226 to 235 Hz. This harmonic tone has an amplitude of approximately 15 dB above the background and corresponds to distant shipping. This feature creates a square of strong correlation from 226 to 235 Hz that is uncorrelated with the surrounding area.

Fig. 6 (a) illustrates the frequency correlation matrix of the ambient noise data in the 1-6000 Hz band, and the corresponding spectrogram is shown in Fig. 6 (b).
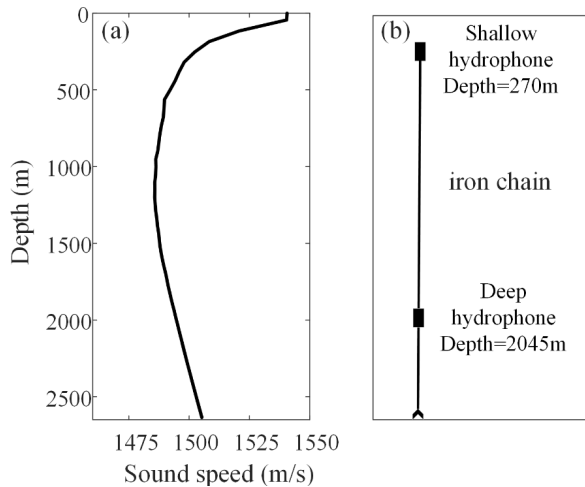
FIGURE 7. (a) Measured sound speed profile and (b) illustration of the receiving system for the experiment in the East China Sea.

FIGURE 8. Wind speed during the experiment.

Strong correlations are observed in the frequency band of 477 to 6000 Hz (the average correlation coefficient in this band is 0.78). It is likely that the noise in this band is predominantly caused by surface wind. Considering this observation in combination with the previous conclusions, it is reasonable to suppose that for the ambient noise recorded in the South China Sea, the principal constituent of the ambient noise in the 477-6000 Hz band is wind-generated noise, while the ambient noise in the band of 155 to 477 Hz is mainly a mixture of wind-generated noise and shipping noise, and the main contributors to the ambient noise below 155 Hz are shipping noise and some unknown noise sources.

B. THE EAST CHINA SEA EXPERIMENT
1) DESCRIPTION OF THE EXPERIMENT AND DATA PROCESSING
Continuous acoustic recordings were collected in the East China Sea from 20 June 2016 to 27 June 2016 at a sampling rate of 16000 Hz. The recorder was deployed in a water depth of 2680 m, with two hydrophones suspended 2410 m and 270 m above the seafloor respectively, as shown in Fig. 7 (b). The water column was characterized by a typical deep ocean sound speed profile, as illustrated in the left of Fig. 7.

A high-pass filter with a cutoff frequency of 50 Hz was applied in the acquisition device. Review of the data revealed no evidence of instrumental problems throughout the recording period; however, most data were contaminated by the impact sounds induced by collisions between the receivers and the iron chain. For this reason, we artificially eliminated these distinct contaminants to obtain 18 hours of relatively pure ambient noise data. Fig. 9 (a) shows the spectrogram for that time period, consisting of 2160 time samples, each of 30 seconds in length. To achieve a high frequency resolution at a relatively low computational cost, the recorded data were first downsampled to 4000 Hz before data analysis, and the spectral levels were then calculated using a Hann-windowed 4000-point discrete Fourier transform with
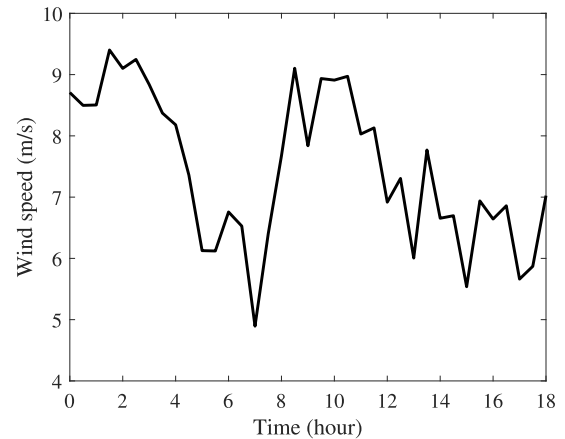
no overlap to produce sequential 30-second power spectrum estimates over the duration of the dataset. With this design, the frequency resolution is 1 Hz, and the time resolution is 30 seconds. During this particular deployment, a relatively strong breeze was blowing at speeds in the range of 5-9.5 m/s (see Fig. 8), with an average wind speed of 7.5 m/s.

2) CORRELATION MATRIX ANALYSIS
Fig. 9 (a) shows the spectrogram for the observed time period. Some clear features of this ambient noise include the impact noise induced by collisions between the receivers and the iron anchor chain, which covers the whole frequency band [region (i) in Fig. 9 (a)]; distant shipping noise, ranging from 283 to 306 Hz between the 1.8th and 9.5th hours [region (ii) in Fig. 9(a)] and from 430 to 450 Hz between the 13.2th and 17.5th hours [region (iii) of Fig. 9 (a)]; and wind-dominated noise above 570 Hz throughout most time segments of the 18-hour analysis window [region (iv) in Fig. 9 (a)].

The frequency correlation matrices for the upper and lower receivers, shown in Fig. 9 (b) and (c), respectively, are characterized by four dominant features. First, from 50 to 100 Hz, a block of strong correlation corresponds to impact noise. The energy of the impact noise is mainly concentrated in the frequency band of 50 to 100 Hz. Some of this energy also extends into the 100 to 2000 Hz band, resulting in a moderate correlation between the 100 to 2000 Hz band and the 50-100 Hz band. Second, the strong correlation block between 100 and 250 Hz corresponds to distant shipping traffic noise; the noise in this band is almost uncorrelated with the noise above 575 Hz, which is dominated by wind-generated noise, indicating that the noise corresponding to the 100 to 250 Hz band is dominated by distant shipping noise. Third, a square region of strong correlation is observed at 250-575 Hz, which is distinct from the second feature. There is a moderate correlation between the 250-575 Hz band and the higher-frequency band dominated by wind-generated noise, implying that the ambient noise in this band is dominated by a mix of distant shipping noise and local wind sources. Both wind sources and shipping sources
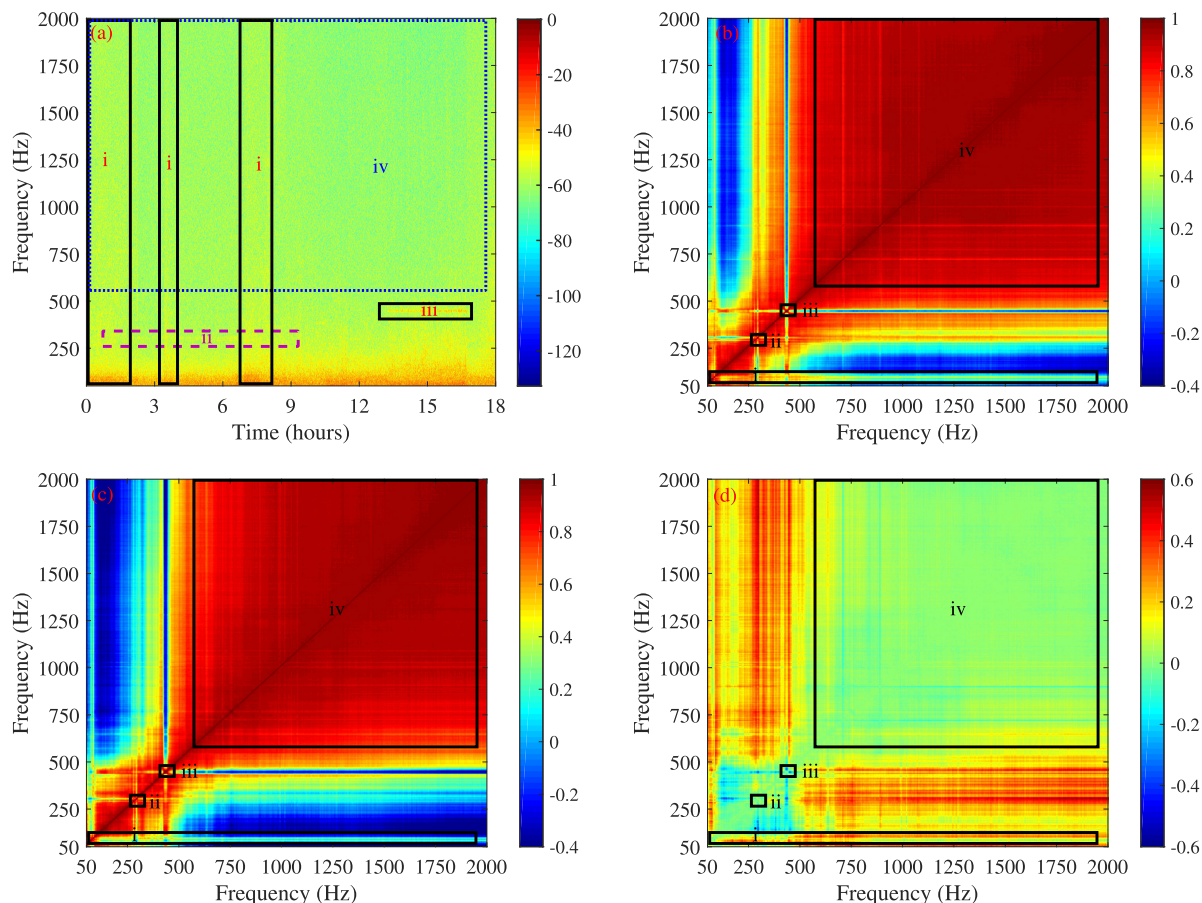
FIGURE 9. (a) Spectrogram of the ambient noise recorded by the upper receiver. (b) Frequency spectrum correlation matrix for the upper receiver. (c) Frequency spectrum correlation matrix for the lower receiver. (d) The difference between the frequency correlation matrices for the upper and lower receivers.

significantly contribute to the noise in this frequency band, and the wind noise sources contribute more to the noise with increasing frequency. Fourth, a region of significantly elevated correlations above 575 Hz corresponds to wind-dominated noise. The strongest correlations are observed between pairs of frequencies in this band (the average correlations in this band are 0.9472 and 0.9415 for the upper and lower receivers, respectively).

To better interpret Fig. 9 (d), we first compared the propagation loss for the wind-generated noise sources and the shipping sources, as shown in Fig. 10 and Fig. 11. One significant difference between these two types of sources is the source depth. For wind-generated noise, the sources are distributed on the sea surface (the corresponding source depth was set to 0.1 m in the simulation). Due to the high bottom loss, distant wind-generated noise suffers high propagation loss and contributes little to the noise field; thus, only local wind-generated sources significantly contribute to the noise field. For shipping noise, the sources are located at a depth near the surface (the corresponding source depth was set to 10 m in the simulation), and the propagation loss is significantly less than that for wind-generated noise, indicating that relatively distant shipping may contribute to the noise field.

The frequency correlation difference matrix in Fig. 9(d) highlights the fact that local wind-generated noise shows a different trend of variation as a function of depth than distantly generated shipping noise does. In the wind-dominated frequency band (the square region at approximately 575 to 2000 Hz), the differences in the frequency correlation coefficients are approximately zero, indicating that the ambient noise intensities at the two receivers at various frequencies may increase or decrease at the same time. In the combined region consisting of a region dominated by wind-generated noise and a mixed region of wind noise and shipping noise (rectangular areas at 250 to 500 Hz and 500 to 2000 Hz), the ambient noise at the upper receiver shows better frequency correlation performance than that at the lower receiver. This phenomenon is mainly due to the different weights of the wind-generated noise in the mixed noise fields at the two receivers. For distant shipping sources, the acoustic energy is mainly concentrated near the bottom of the ocean in the experimental environment, as shown in Fig. 11 (a) and (b), but wind activity contributes more to the soundscape at the upper receiver than at the lower receiver. This results in weaker correlations at the lower receiver than at the upper receiver in these rectangular areas because wind-generated noise is
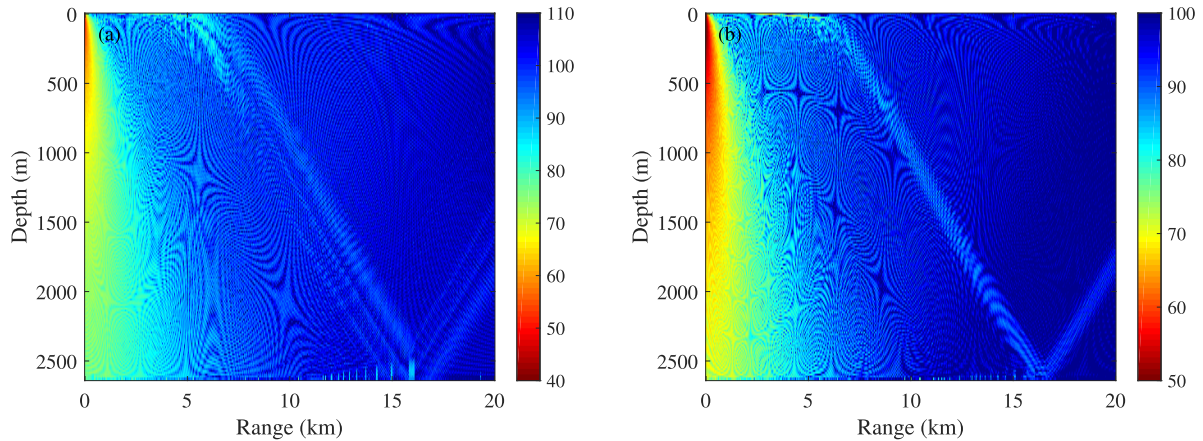
FIGURE 10. Propagation loss for a point source located at 0.1 m in depth (modeling a wind-generated noise source) for frequencies of (a) 250 Hz and (b) 450 Hz. Bottom compressional wave speed of 1600 m/s, bottom density of 1.8 g/cm^3, and bottom attenuation of 0.8 dB/λ were used in the simulation.
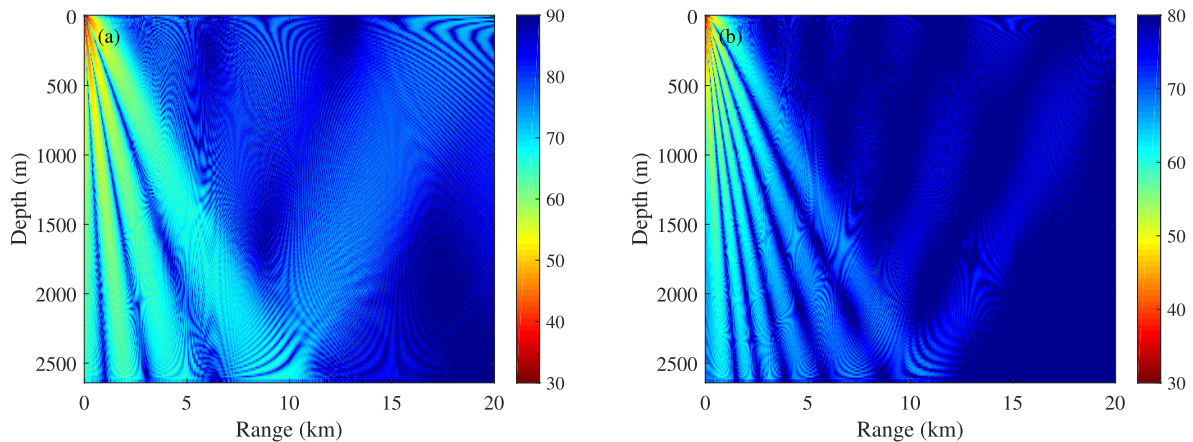

FIGURE 11. Propagation loss for a point source located at 10 m in depth (modeling a ship noise source) for frequencies of (a) 250 Hz and (b) 450 Hz. Bottom compressional wave speed of 1600 m/s, bottom density of 1.8 g/cm^3, and bottom attenuation of 0.8 dB/λ were used in the simulation.

generally uncorrelated with distant shipping noise. In the shipping-dominated region and the mixed region of shipping noise and wind-generated noise (square regions at approximately 100 to 500 Hz), the frequency correlation differences are slightly less than zero, implying that the correlations of the ambient noise at the lower receiving depth are slightly different from those at the upper receiving depth. This phenomenon may be attributed to the differences in the propagation loss for distant shipping sources at different receiving depths and frequencies.

To illustrate the effect of the wind speed on the frequency correlation characteristics, the ambient noise was divided into two groups: one group corresponding to wind speeds less than 7.5 m/s (defined as low wind conditions) and another group corresponding to wind speeds greater than 7.5 m/s (defined as high wind conditions). Both groups have a duration 8 hours of data. The frequency correlation matrices for high wind conditions and low wind conditions are presented in Fig. 12 (a) and (b), respectively. These frequency correlation matrices were then subtracted from each other to find the correlation difference matrix between high wind

conditions and low wind conditions, as shown in Fig. 12 (c). It is evident from Fig. 12 (a) and (b) that the ambient noise spectral levels are highly correlated in the band of 575 to 2000 Hz, and the average correlation coefficient values are 0.9496 and 0.8902 for high wind speeds and low wind speeds, respectively, indicating that the wind-generated noise is the main constituent in this frequency band. Notably, several "plus-sign"-shaped correlation features are contained within the frequency band of the wind-dominated frequency region, labeled (i) in Fig. 12; these features are induced by the narrowband noise radiated by distant discrete shipping traffic. In the vicinity of the diagonal lines, the frequency correlation differences approach zero because the elements adjacent to the diagonal are always approximately equal to unity under any wind conditions. For other frequency regions (except for the plus-sign region), the frequency correlation differences are slightly greater than zero, indicating that the correlations are increased under high wind conditions compare with low wind conditions. The higher frequency correlations for high wind conditions can likely be attributed to the increase in the contribution of the wind noise component to the overall
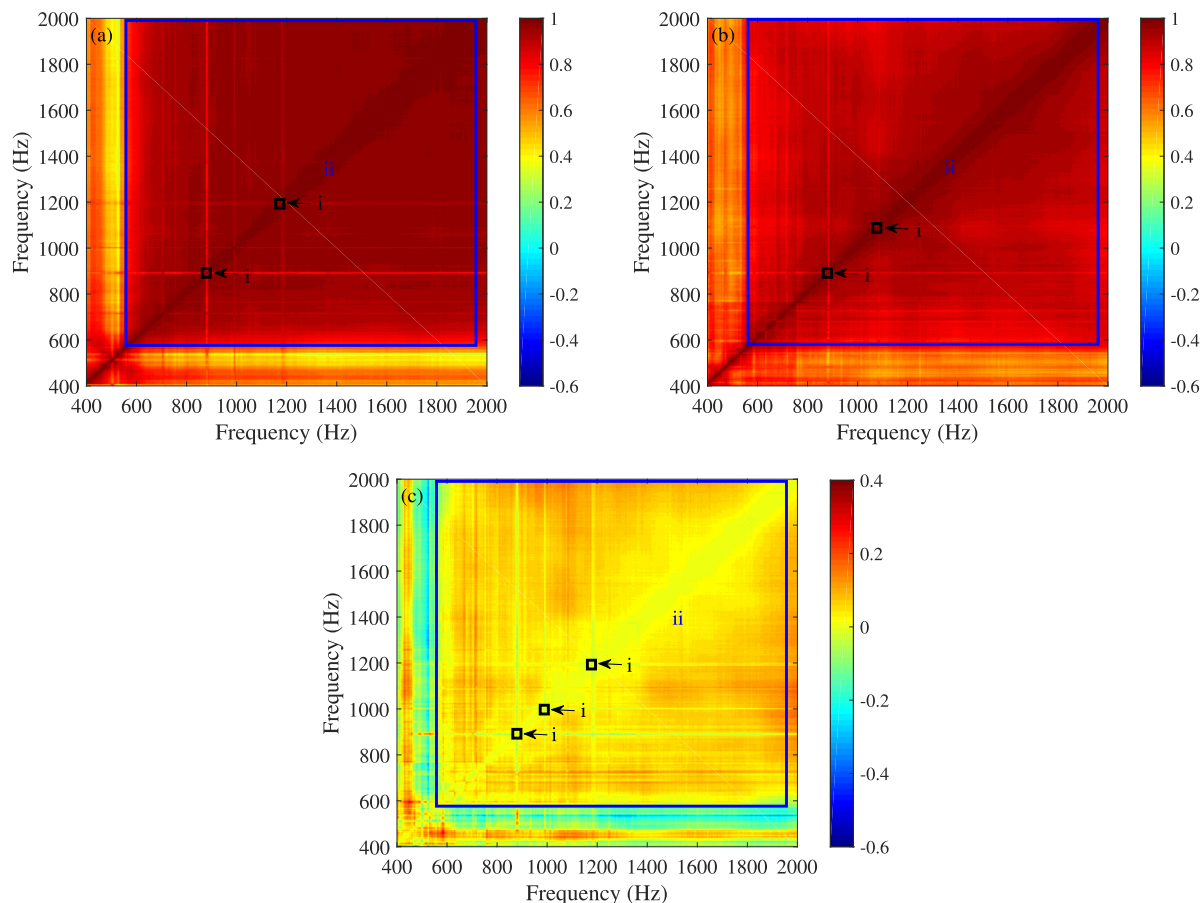
FIGURE 12. Frequency correlation matrices for (a) high wind speeds and (b) low wind speeds. (c) Frequency correlation difference matrix derived by taking the point-by-point differences between the frequency correlation matrices for high wind conditions and low wind conditions.

soundscape under high wind conditions compared with low wind conditions.

IV. CONCLUSION

Frequency correlation matrix analysis was performed on ambient noise data recorded in the South China Sea and the East China Sea to quantify the predominant sources driving the noise levels in different frequency regions. The wind-dominated and shipping-dominated frequency regions as well as the mixed regions combining both types of noise sources were identified. In addition, the frequency correlation characteristics at different receiving depths and under different wind conditions were compared and investigated.

For the ambient noise recorded in the South China Sea, the correlation coefficients between the noise levels in pairs of frequency bands were calculated, and the correlation plots showed distinct boxes of high correlation with high contrast relative to the uncorrelated regions of the spectrum. These boxes were used to identify the regions dominated by various noise sources. During the observation window, the wind noise was the absolute principal constituent above 477 Hz, the ambient noise was dominated by a weighted mixture of the wind noise and shipping noise in the band of 155-477 Hz,

and the ambient noise was dominated by an unknown source mechanism below 155 Hz.

For the ambient noise recorded in the East China Sea, the correlation matrices at upper and lower receiving depths were compared. The analysis demonstrated that local wind-generated noise change as a function of depth compared to distantly generated shipping noise. In the wind-dominated region, the correlations of the ambient noise at the upper receiver are almost identical to those at the lower receiver, unlike in the shipping-noise dominated region. In addition, the wind-dominated noise region is better correlated with the mixed noise region at the upper receiving depth than at the lower receiving depth because the wind noise component accounts for a greater percentage of the overall noise at the upper receiver than at the lower receiver. The use of correlation matrices to analyze the influence of wind speed on the noise spectral level correlations in the wind-dominated frequency band was further demonstrated by computing the correlation matrices for two groups of noise spectra, grouped by two different surface wind speed categories. The correlation matrices for data recorded under low wind speed conditions and high wind speed conditions were compared, and the results indicate that the wind-dominated noise was

better correlated under high wind conditions than low wind conditions.

ACKNOWLEDGMENT

The authors thank the staff involved in the acoustic research experiment in China Sea.

REFERENCES

[1] W. M. Carey and R. B. Evans, *Ocean Ambient Noise: Measurement and Theory*. Springer, 2011, pp. 52–162.

[2] Y. Wu, H. Zhao, and W. Xu, "Sound transmission loss correction due to hydrophone fluctuation with propagation model," in *Proc. OCEANS*, May 2015, pp. 1–6.

[3] J. A. Colosi, T. F. Duda, Y.-T. Lin, J. F. Lynch, A. E. Newhall, and B. D. Cornuelle, "Observations of sound-speed fluctuations on the New Jersey continental shelf in the summer of 2006," *J. Acoust. Soc. Amer.*, vol. 131, no. 2, pp. 1733–1748, Feb. 2012.

[4] D. Jourdain, "High frequency signal fluctuations in shallow water propagation," in *Proc. OCEANS*. vol. 2, Dec. 2002, pp. 278–283.

[5] Q. Zhang, X. Guo, and L. Ma, "The research of the characteristics of the ocean ambient noise under varying environment," *J. Comp. Acous.*, vol. 25, no. 2, Jun. 2017, Art. no. 1750021.

[6] Q. Yang, K. Yang, C. Huang, Y. Zhang, X. Zhou, R. Xue, and H. Liu, "Experimental investigation of oceanic ambient noise generated by typhoon in deep ocean," in *Proc. OCEANS*, Marseille, France, Jun. 2019, pp. 1–4.

[7] J. H. Wilson, "Wind-generated noise modeling," *J. Acoust. Soc. Amer.*, vol. 73, no. 1, pp. 211–216, 1983.

[8] J. Berger, J. R. Bidlot, M. A. Dzieciuch, W. E. Farrell, P. F. Worcester, and R. A. Stephen, "A deep ocean acoustic noise floor, 1-800 Hz," *J. Acoust. Soc. Amer.*, vol. 143, no. 2, p. 1223, 2018.

[9] F. Li, D. Xu, J. Wang, and W. Luo, "Observations of wind-generated noise by the tropical cyclone," *J. Acoust. Soc. Amer.*, vol. 143, no. 6, pp. 3312–3324, Jun. 2018.

[10] D. R. Barclay and M. J. Buckingham, "Depth dependence of wind-driven, broadband ambient noise in the Philippine Sea," *J. Acoust. Soc. Amer.*, vol. 133, no. 1, pp. 62–71, Jan. 2013.

[11] Y. Huang, Q. Ren, and T. Li, "A geometric model for the spatial correlation of an acoustic vector field in surface-generated noise," *J. Mar. Sci. Appl.*, vol. 11, no. 1, pp. 119–125, Mar. 2012.

[12] F. Liufang, "A study of characteristics of ocean ambient noise based on fiber optic vector hydrophone," Nat. Univ. Defense Technol., Tech. Rep., Hunan, China, 2013.

[13] A. Gontz, L. Hatch, D. Wiley, and E. Remillard, "Shallow-water seismic surveys—How much noise are we introducing into the ocean?" in *Proc. OCEANS*, Sep. 2006, pp. 1–5.

[14] B. Olofsson, "Marine ambient seismic noise in the frequency range 1–10 Hz," *Lead. Edge*, vol. 29, no. 4, pp. 418–435, Apr. 2010.

[15] D. G. Albert and S. N. Decato, "Acoustic and seismic ambient noise measurements in urban and rural areas," *Appl. Acoust.*, vol. 119, pp. 135–143, Apr. 2017.

[16] T. Tonegawa, Y. Fukao, T. Takahashi, K. Obana, S. Kodaira, and Y. Kaneda, "Ambient seafloor noise excited by earthquakes in the Nankai subduction zone," *Nature Commun.*, vol. 6, no. 1, May 2015.

[17] G. B. Deane and M. D. Stokes, "Model calculations of the underwater noise of breaking waves and comparison with experiment," *J. Acoust. Soc. Amer.*, vol. 127, no. 6, pp. 3394–3410, Jun. 2010.

[18] A. Brown, J. Thomson, A. Ellenson, F. T. Rollano, H. T. Ozkan-Haller, and M. C. Haller, "Kinematics and statistics of breaking waves observed using SWIFT buoys," *IEEE J. Ocean. Eng.*, vol. 44, no. 4, pp. 1011–1023, Oct. 2019.

[19] S. L. Means and R. M. Heitmeyer, "Low-frequency sound generation by an individual open-ocean breaking wave," *J. Acoust. Soc. Amer.*, vol. 110, no. 2, pp. 761–768, Aug. 2001.

[20] J. Lin, P. Jiang, B. Yin, J. Li, and L. Ma, "Effects of source distribution in depth on ocean ambient noise field," *AIP Conf. Proc.*, vol. 1495, p. 544, Nov. 2012.

[21] I. Benjaminsen, C. E. Solberg, and D. Tollefsen, "Shipping and seismic exploration contributors to noise in the northern Norwegian sea: Trends and recent measurements," in *Proc. Meetings Acoust. (ECUA)*, vol. 17, no. 1. Alexandria, VA, USA: ASA, 2012, Art. no. 070033.

[22] G. V. Frisk, "Noiseonomics: The relationship between ambient noise levels in the sea and global economic trends," *Sci. Rep.*, vol. 2, no. 1, p. 437, Dec. 2012.

[23] N. R. Chapman and A. Price, "Low frequency deep ocean ambient noise trend in the Northeast Pacific ocean," *J. Acoust. Soc. Amer.*, vol. 129, no. 5, pp. EL161–EL165, May 2011.

[24] C. Erbe, A. Macgillivray, and R. Williams, "Mapping cumulative noise from shipping to inform marine spatial planning," *J. Acoust. Soc. Amer.*, vol. 132, no. 5, pp. EL423–EL428, Nov. 2012.

[25] N. D. Merchant, P. Blondel, D. T. Dakin, and J. Dorocicz, "Averaging underwater noise levels for environmental assessment of shipping," *J. Acoust. Soc. Amer.*, vol. 132, no. 4, pp. EL343–EL349, Oct. 2012.

[26] H. Li, L. Zheng-Lin, Z. Ren-He, and P. Zhao-Hui, "Horizontal correlation of ambient noise near a sea route," *Chin. Phys. Lett.*, vol. 25, no. 2, pp. 582–585, Feb. 2008.

[27] M. Friendly, "Corrgrams: Exploratory displays for correlation matrices," *Amer. Statistician*, vol. 56, no. 4, pp. 316–324, Nov. 2002.

[28] L. J. Frasinski, K. Codling, and P. A. Hatherly, "Covariance mapping: A correlation method applied to multiphoton multiple ionization," *Science*, vol. 246, no. 4933, pp. 1029–1031, Nov. 1989.

[29] D. J. Fenn, M. A. Porter, S. Williams, M. Mcdonald, N. F. Johnson, and N. S. Jones, "Temporal evolution of financial-market correlations," *Phys. Rev. E, Stat. Phys. Plasmas Fluids Relat. Interdiscip. Top.*, vol. 84, no. 2, Aug. 2011, Art. no. 026109.

[30] R. H. Nichols and C. E. Sayer, "Frequency-frequency correlations of ocean ambient noise levels," *J. Acoust. Soc. Amer.*, vol. 61, no. 5, pp. 1188–1190, May 1977.

[31] K. R. Curtis, B. M. Howe, and J. A. Mercer, "Low-frequency ambient sound in the North Pacific: Long time series observations," *J. Acoust. Soc. Amer.*, vol. 106, no. 6, pp. 3189–3200, Dec. 1999.

[32] S. Nichols and D. Bradley, "Methods for identifying source mechanisms in the low-frequency deep-ocean ambient noise field," in *Proc. Underwater Acoust. Conf. Exhib.*, 2013.

[33] S. Nichols and D. L. Bradley, "Wind-dependence of low-frequency ambient noise in the deep-ocean sound channel," *J. Acoust. Soc. Amer.*, vol. 133, no. 5, p. 3396, May 2013.

[34] S. Nichols and D. Bradley, "Using correlation matrices to identify temporal characteristics of ambient noise," in *Proc. Underwater Acoust. Conf. Exhib.*, 2014.

[35] D. L. Bradley and S. Nichols, "Worldwide low-frequency ambient noise," *Acoust. Today*, vol. 11, no. 1, pp. 20–26, 2015.

[36] J. L. Miksis-Olds and S. M. Nichols, "Is low frequency ocean sound increasing globally?" *J. Acoust. Soc. Amer.*, vol. 139, no. 1, pp. 501–511, Jan. 2016.

[37] S. M. Nichols and D. L. Bradley, "Use of noise correlation matrices to interpret ocean ambient noise," *J. Acoust. Soc. Amer.*, vol. 145, no. 4, pp. 2337–2349, Apr. 2019.

[38] G. M. Wenz, "Acoustic ambient noise in the ocean: Spectra and sources," *J. Acoust. Soc. Amer.*, vol. 34, no. 12, pp. 1936–1956, Dec. 1962.

JIANBO ZHOU received the B.S. and Ph.D. degrees in underwater acoustic engineering from the School of Underwater Acoustic Engineering, Harbin Engineering University, Harbin, China, in 2013 and 2018, respectively. He currently holds a postdoctoral position with the Department of Acoustic and Information Engineering, School of Marine Science and Technology, Northwestern Polytechnical University. His current research interests include modeling and the application of ocean ambient noise and related fields.

● ● ●